

Article

Energy Saving and Thermal Comfort Performance of Passive Retrofitting Measures for Traditional Rammed Earth House in Lingnan, China

Shihao Li ¹, Meilin Wang ¹ , Pengyuan Shen ^{1,*} , Xue Cui ², Linqian Bu ¹, Ruji Wei ¹, Longzhu Zhang ¹ and Chengjia Wu ¹

¹ School of Architecture, Harbin Institute of Technology, Shenzhen 518055, China

² Department of Building and Real Estate, Faculty of Construction and Environment, The Hong Kong Polytechnic University, Hong Kong, China

* Correspondence: pengyuan_pub@163.com; Tel.: +86-13764602660

Abstract: The traditional rammed earth houses sharing similar patterns in the Lingnan region, south China, and distributed in rectangular arrays, are gradually losing their vitality and becoming uninhabited under modern living conditions. This research examined a typical pattern called the “Four-point gold” house and analyzed the suitability of different retrofitting technologies by field measurements and building simulation. To optimize energy consumption, indoor thermal comfort, and the corresponding economic performance of the retrofitting measures for the prototypical house, five measures, including wall insulation, reflective roof coating, carpet, sunshade, and natural ventilation, are proposed after considering the status quo of the building envelope. It is found that the best performance in energy-saving, dynamic investment payback period, and annual indoor thermal comfort are 2192.27 kWh/a, 9.17 years, and 1766 h, respectively. Different parameters are included to be clustered by K means clustering technique, and the comprehensively optimized scheme consists of a regime of 30 mm XPS 30 mm, ZS-221 white coating, carpet, 0.5 m sunshade width, and turning off windows (doors). The proposed retrofitting strategy can be promoted to a wide range of traditional rammed earth houses in the Lingnan region in China and holds a conspicuous energy-saving potential for the suburban and rural residential sectors in the region.

Keywords: rammed earth house; indoor thermal comfort; building retrofit; clustering technique



Citation: Li, S.; Wang, M.; Shen, P.; Cui, X.; Bu, L.; Wei, R.; Zhang, L.; Wu, C. Energy Saving and Thermal Comfort Performance of Passive Retrofitting Measures for Traditional Rammed Earth House in Lingnan, China. *Buildings* **2022**, *12*, 1716. <https://doi.org/10.3390/buildings12101716>

Academic Editor: Benedetto Nastasi

Received: 8 September 2022

Accepted: 13 October 2022

Published: 17 October 2022

Publisher's Note: MDPI stays neutral with regard to jurisdictional claims in published maps and institutional affiliations.



Copyright: © 2022 by the authors. Licensee MDPI, Basel, Switzerland. This article is an open access article distributed under the terms and conditions of the Creative Commons Attribution (CC BY) license (<https://creativecommons.org/licenses/by/4.0/>).

1. Introduction

Rammed earth refers to a compacted mixture of mud blocks that are strong, dense, and have few gaps. It is used as a construction material and has very strong plasticity [1]. Since the 1970s, different groups around the world have begun to conduct scientific research on the properties of rammed earth [2]. Compared with conventional building materials, rammed earth is low-cost, readily available, recyclable, and considered environmentally friendly and sustainable [3], especially when the material is locally available [4,5]. Rammed earth building has good thermal performance under specific climatic and technical conditions [6]. This is due to its high thermal inertia [7] and good thermal insulation performance [8]. Rammed earth buildings do not need too much external energy input throughout the year [9], and indoor thermal comfort can be achieved during most of the time of the year [3,7]. In addition, it has been shown that due to its good bioclimatic properties, an earth envelope can lead to a reduction in energy used for heating, cooling, and humidity control [10]. In general, the quality of the indoor thermal environment in summer can be acceptable [11,12]. The comfortable time can be extended when other design measures, such as insulation, double glazing, shading, and ventilation, are taken into account [11,13]. Small and large window shadings lead to lower energy loads in the torrid-arid area [14]. Moreover, the results of the research show that a combination of large

compacted earth walls, nighttime cross ventilation, and overhangs can effectively reduce the energy demand for space cooling [15]. However, thermal comfort in winter cannot be fully achieved without heating [12,13]. Thus, it is possible to archive acceptable comfort conditions by passive means [16–19], which contributes to reducing the heating/cooling energy demand of the traditional rammed earth buildings [20–22].

What is more, historical and traditional rammed earth houses in Lingnan account for a large part of the existing building stock, and they are quite distributed in the region inhabited by the clans in the Chaoshan area.. There are mainly two styles of “climbing lion” and “Four-point gold”, which are generally distributed in a rectangular array [23]. As shown in Figure 1, the “Climbing lion” house looks like a lion poised to climb. The gate indicates its mouth, the two small rooms are the front claws, the hall is the belly, and the two other bedrooms on the sides of the hall are the rear claws. “Four-point gold” has two extra rooms near the gate compared with the “Climbing lion” house. The shape is like the Chinese character ‘金’ (gold) and can be seen in Figure 2. Therefore, the architectural styles in traditional villages are the same and arranged in the same direction, and “cold lanes” are formed between buildings [24,25]. Research has shown that the residents in Tulou (earth building) had better satisfaction with the indoor thermal environment and overall indoor environmental quality than residents in normal rural buildings [26]. Building integrated photovoltaic was employed to optimize the solar energy application on the rooftop of traditional Lingnan buildings [27]. However, there are few studies on the indoor thermal environment and energy-saving renovation of rammed earth houses in Lingnan, and there are no rules, norms, or standards for reference [28].

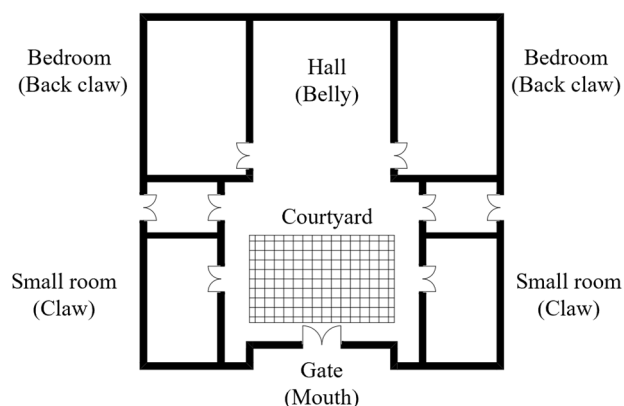


Figure 1. Archaic “climbing lion” rammed earth house.

The industrialization of the construction industry (materials, systems, etc.) led to the standardization of buildings. The performance of traditional buildings can gradually deteriorate over time. As a consequence, they became more dependent on heating, ventilation, and air conditioning (HVAC) systems to cater to thermal comfort requirements, which resulted in energy use that was not a necessity in previous vernacular buildings. This situation led to the disregard for the vernacular wisdom in passive design, changing not only the way buildings and indoor spaces were designed (commonly arranged by function and thermal needs) but also the occupants’ living habits [29]. Coupled with the outflow of the rural population in China due to the urbanization process, many traditional rammed earth houses are now uninhabited. Traditional buildings are gradually abandoned by the descendants of their original residents in the process of modernization.

Therefore, the investigation of Lingnan rammed earth houses is not only conducive to the protection and inheritance of historical buildings but also of great significance to the sustainable development of society. In this study, the indoor and outdoor thermal environment parameters of the traditional rammed earth house “Four-point gold” in Lingnan were tested. The building model is established using DesignBuilder and calibrated by onsite measured data. Then the thermal performance of the rammed earth house is analyzed,

and the passive energy-saving measures are put forward. Finally, the corresponding optimal scheme for each optimization objective and the comprehensively optimal scheme are proposed by the orthogonal experiment method. This research helps to better understand the characteristics of rammed earth houses in the Lingnan region and provides technical support for energy saving in the residential sector. It is anticipated that the renovation measures can be applied to not only the prototypical building in this research but also to the rammed earth buildings in the region so that these traditional houses in Lingnan will have the chance to rejuvenate in terms of modern living conditions and continue to maintain vitality in the future.

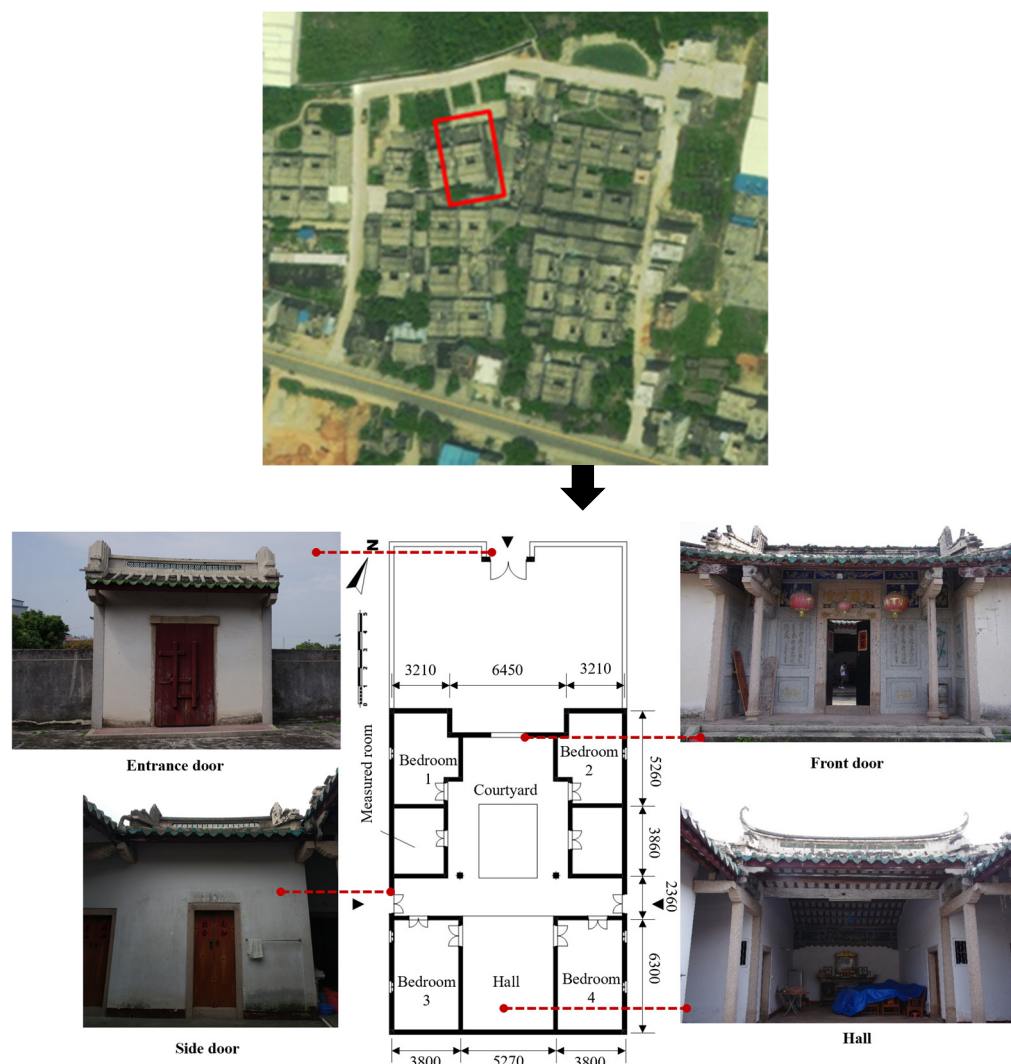


Figure 2. Location, status quo and the floor plan of the “Four-point gold” house.

2. Methods

2.1. Field Survey

This study selected a house in Jieyang, Guangdong Province, located in the north of Xinzhezai. There are 14 “climbing lion” and 13 “Four-point gold” houses in this village. The “Four-point gold” houses are the target prototype in this research. Its floor plan and locations are shown in Figure 2. The house retains the traditional Lingnan architectural styles. The archaic rammed earth technique of Chaoshan is adopted, which is made of red mud, coarse sand, and other materials. The top of the wall directly supports the wooden beams, and the rooftop is covered with tiles. The overhanging eaves in front of the hall are undertaken by stone pillars in front of the courtyard. There are walls on the periphery

of the building. Behind the entrance door, there lays the front hall, and the rooms on the left and right side are the front rooms (bedrooms). Further ahead is a courtyard, and the rooms on both sides are the kitchen and utility room. On the other side of the courtyard, a multifunctional space with a large room on each side (bedroom) is designed. The large room is divided into two floors by a wooden partition, and the attics are used for storage. Influenced by the traditional concept of “withholding wealth”, “Four-point gold” generally does not open windows to the outside but only openings to the inner courtyard. The house only has external windows on the east and west sides, which is limited by the strength of the rammed earth walls. The window-to-wall ratios of the east and west external walls of the bedrooms are 0.017 and 0.011, according to onsite measurements.

2.2. Onsite Test

Field measurements and investigations were conducted from 2–9 March in winter and from 12–30 July in summer in 2019. The indoor temperature, relative humidity, and black bulb temperature were tested by HOBO temperature and humidity and the global temperature meter. The detailed parameters of the instruments are shown in Table 1. To ensure the accuracy of the tested data, the room was not occupied during the measurement period. Doors and windows are closed to test the condition without natural ventilation. The thermal environment of the utility room and hall was measured and monitored, as shown in Figure 3.

Table 1. The parameters of the measurement equipment used.

Equipment	Specification	Measurement Range	Accuracy
HOBO temperature and humidity recorder	U12-012	temperature: $-20\sim 70\text{ }^{\circ}\text{C}$ relative humidity: 5~95%	$\pm 2.5\%$
Global temperature recorder	testo480	$-20\sim +80\text{ }^{\circ}\text{C}$	$\pm 0.3\text{ }^{\circ}\text{C}$

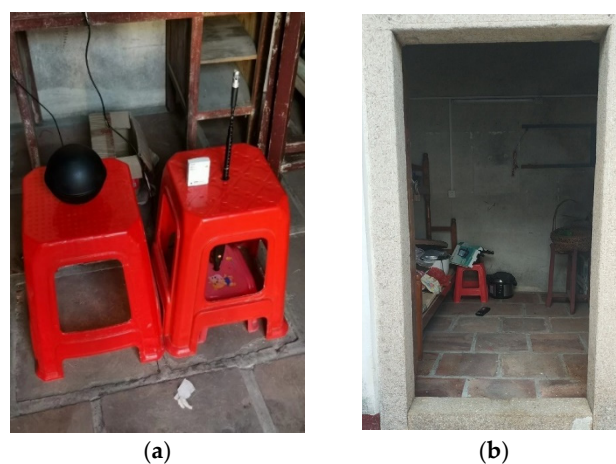


Figure 3. Instruments and their layouts: (a) Hall; (b) Utility room.

2.3. Building Simulation Model

The indoor environment and energy-saving effect of various retrofitting measures were simulated by DesignBuilder, which uses EnergyPlus as the simulation engine and energy use analysis. According to the onsite investigation, the geometric information of the house was collected and fed into DesignBuilder. As shown in Figure 4, the building has two stories with wide eaves, which can effectively shade and ensure ventilation and daylight in the courtyard. We manually tuned the model to fit the simulation results to the onsite measurements as model calibration. The calibrated thermophysical properties

of building walls, roofs, and floors are shown in Table 2. The thermal resistance of the rammed earth wall is $0.57 \text{ m}^2 \cdot \text{K}/\text{W}$, which is higher than that of the tile roof and concrete floor. This research only considers the basic structure of the building due to its simple interior furnishings. There is no larger appliance, so the model does not account for heat loads other than lamps. An occupancy intensity of two people per bedroom is assumed, and the bedrooms are not used during 9:00–22:00. Due to the aging of the house and poor airtightness of doors and windows, the air infiltration of the house is calibrated to be 3.5 h^{-1} . Currently, the house is not equipped with an HVAC system. We propose a simple packaged terminal heat pump system for the building to meet the requirement of thermal comfort in the simulation. The parameters of the HVAC system are listed in Table 3. The cooling temperature is $25 \text{ }^\circ\text{C}$, and the heating temperature is $18 \text{ }^\circ\text{C}$. Location coordinates and meteorological parameters are also input parameters.

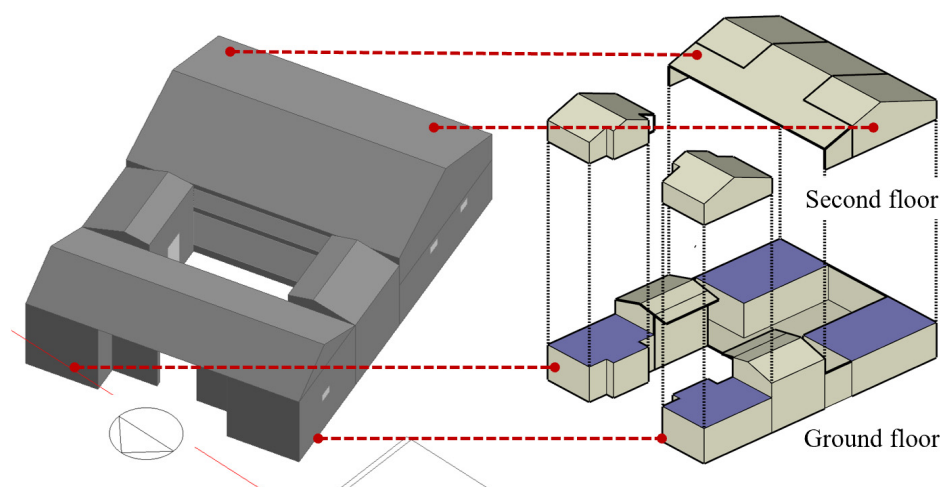


Figure 4. A 3D model of the house.

Table 2. Thermophysical properties of the building envelope.

Structure	Heat Transfer Coefficient/ $\text{W}/(\text{m}^2 \cdot \text{K})$	Thermal Resistance/ $(\text{m}^2 \cdot \text{K}/\text{W})$	Thickness /m
Rammed earth wall	1.754	0.570	0.24
Roof	2.790	0.358	0.3
Floor	2.098	0.477	0.3

Table 3. Parameters of the packaged terminal heat pump system.

Parameters	Values
Design indoor temperature in winter	$18 \text{ }^\circ\text{C}$
Design indoor temperature in summer	$25 \text{ }^\circ\text{C}$
Heat Pump Heating Coil Gross Rated COP	2.75
Cooling Coil Gross Rated COP	3
Operational time	22:00–9:00
Meteorological parameters	Typical meteorological year data of Shantou
Air infiltration	3.5 h^{-1}
Indoor thermal disturbance	People and lighting

Retrofitting measures could be put forward through the analysis of original building's heat transfer and indoor thermal environment. The corresponding thermophysical parameters of the measures are new inputs to simulate energy consumption and thermal comfort. The best retrofitting scheme can be found according to the characteristics of low HVAC system energy consumption, long comfortable period, and short dynamic investment

payback period. Orthogonal experimental method is adopted to select suitable scheme with evenly dispersed study cases. Each average of sensitivity index ($\overline{K_{jm}}$) is the average experimental index of the corresponding cases with same retrofitting measure (factor j) and level (m), which can evaluate the performance of the measures. Maximum difference (R_j) of retrofitting measures is the difference between maximum and minimum $\overline{K_{jm}}$. Higher R_j indicates more sensitivity of the specific retrofitting measure.

2.4. Dynamic Investment Payback Period

For building energy-saving retrofitting, economic evaluation is important to the feasibility of the renovation project. The payback period, incremental cost, and net present value are the usually used indicators of economic analysis. Incremental cost refers to the direct and indirect costs caused by transformation, including materials, construction measures, machinery, and labor costs. The dynamic payback period is used for economic analysis, as shown in Equations (1) and (2). The discount rate is 8% when that is calculated [30].

$$NPV = \sum_{t=1}^n \frac{C_t}{(1+r)^t} - C_0 \quad (1)$$

$$\Delta P_t = (N-1) + \frac{|A_{N-1}|}{C_N} \quad (2)$$

where NPV refers to the net present value of year t , n refers to the calculation cycle, r refers to the discount rate, C_t refers to cash flow in year t , C_0 refers to initial incremental investment cost, ΔP_t refers to the dynamic investment payback period, N refers to the year of cumulative net cash flow first becoming positive, A_{N-1} refers to the cumulative net cash flows with the last negative item, C_N refers to the cumulative net cash flow of year N .

2.5. K-Means Clustering Based Decision Making

In this study, a combined indicator of building energy consumption, payback period, and indoor thermal comfort was used to evaluate the combined performance of different energy efficiency retrofit measures. However, since energy consumption, payback period, and indoor thermal comfort have different unit systems, it is not possible to further evaluate the merits of the optimized measures. Therefore, the K-means clustering method [31] was used to make the different optimization target values dimensionless and facilitate the comparative analysis of the integrated indexes. By clustering, the experimental results of the three optimization objectives were classified into 11 categories. The degree of merit of the categories is expressed by the magnitude of their values, i.e., measures with higher value have better improvement effects. The composite index is the sum of the values of the improvement targets corresponding to the clustering categories, and the final optimization scheme can be determined by assessing the magnitude of the composite index.

3. Building Simulation Results

3.1. Model Validation

3.1.1. Winter

As shown in Figure 5, from 3–9 March, the overall outdoor temperature showed a downward trend. The maximum outdoor temperature was 25.13 °C, and the lowest temperature was 13.38 °C on 8 March. The average and minimum indoor temperatures are 18.7 °C and 16.3 °C, fluctuating with the outdoor temperature, and this is able to create a comfortable indoor thermal environment most of the time. The variation trend of the indoor global temperature is consistent with the indoor temperature, but that is always slightly higher than the indoor air temperature. The air temperature in the hall is almost the same as the ambient temperature, and the global temperature in the hall is also slightly higher than the hall temperature. Due to the strong solar radiation intensity on the 13th and 14th, and the semi-open structure of the hall, the global temperature was significantly higher than the air temperature, while that was still slightly higher than the air temperature

in the measured room. As shown in Figure 5b, the indoor relative humidity ranges from 71.9% to 87.7%. Even in winter, the ambient relative humidity is high, with an average of 93.94%. The calibrated model can accurately simulate indoor temperature in winter. The difference between the simulated indoor temperature and the measured temperature is very small, and the average absolute error is only 0.47 °C with an average relative error of 2.51%. With the change of time, the simulated indoor relative humidity has roughly the same trend as the measured value. On the 3rd, 4th, and 9th, the model showed relatively higher accuracy. During other time periods, the absolute error of this model is relatively large, but the mean absolute error is still well controlled at 5.76%, and the mean relative error is 8.22%.

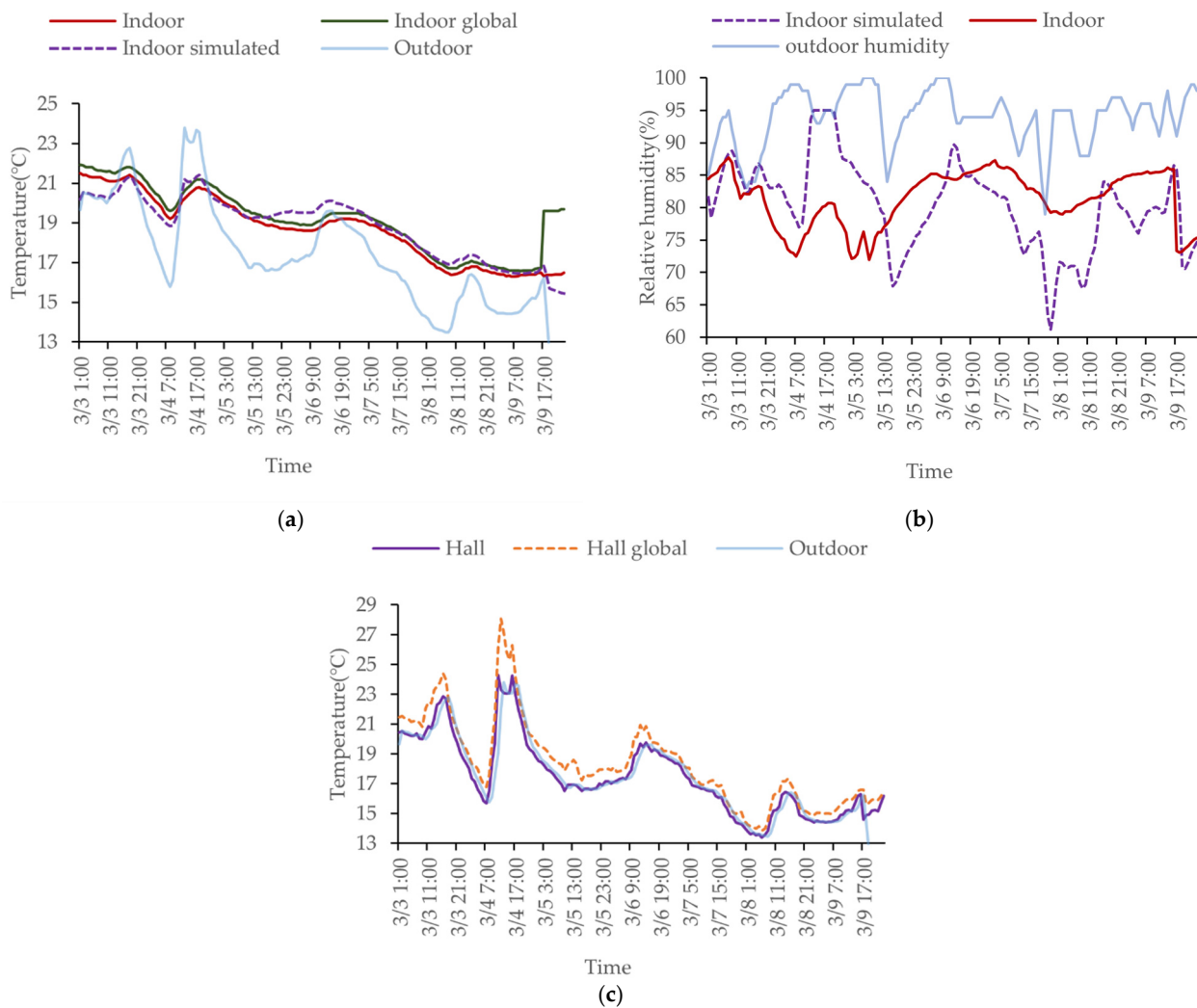


Figure 5. Comparison of measured and simulated values in winter: (a) Indoor temperature; (b) Indoor relative humidity; (c) hall temperature.

3.1.2. Summer

The measured and simulated temperatures from 17–30 July are shown in Figure 6a,c. It can be seen that the highest outdoor air temperature can reach 37.4 °C, the average value is 29.25 °C, and the daily temperature variation is large. During the day, due to the thermal resistance and thermal inertia of the envelope, the peaks of the hall temperature and indoor temperature are lower and delayed compared with the outdoor air temperature, but the average temperatures of them are 30.39 °C and 30.36 °C, respectively. However, on 21, 23, and 30 July, the peak air temperature of the hall was slightly higher than the outdoor air temperature. This was due to the thermal inertia of the house itself not reducing

the air temperature as quickly as the rain did to the outdoor air. The wind speed was about 0.7 m/s at that time, so the heat accumulated inside the hall was dissipated slowly, resulting in higher air temperature. The air temperature at night is lower than the indoor air temperature, thanks to night flushing. The indoor global temperature is slightly higher than the air temperature, and the peak values of the hall are also significantly higher than that of the indoor. As shown in Figure 6b, the city of Puning has high humidity in summer. Even on sunny days, the outdoor relative humidity can reach about 90%, and the daily humidity fluctuates greatly. Although the hall is a semi-open space, the humidity change trend is quite different from that of the outdoors. The outdoor humidity peak usually occurs at 20:00–22:00, while the maximum humidity in the hall occurs at dawn. Since the doors and windows are closed, the indoor humidity changes are relatively less affected by the outdoor humidity, and the relative humidity fluctuates between 70% and 90%. After the rain from the 21st to the 30th, the indoor relative humidity was mostly above 80%. In such high humidity, people are more likely to feel stuffy in summer.

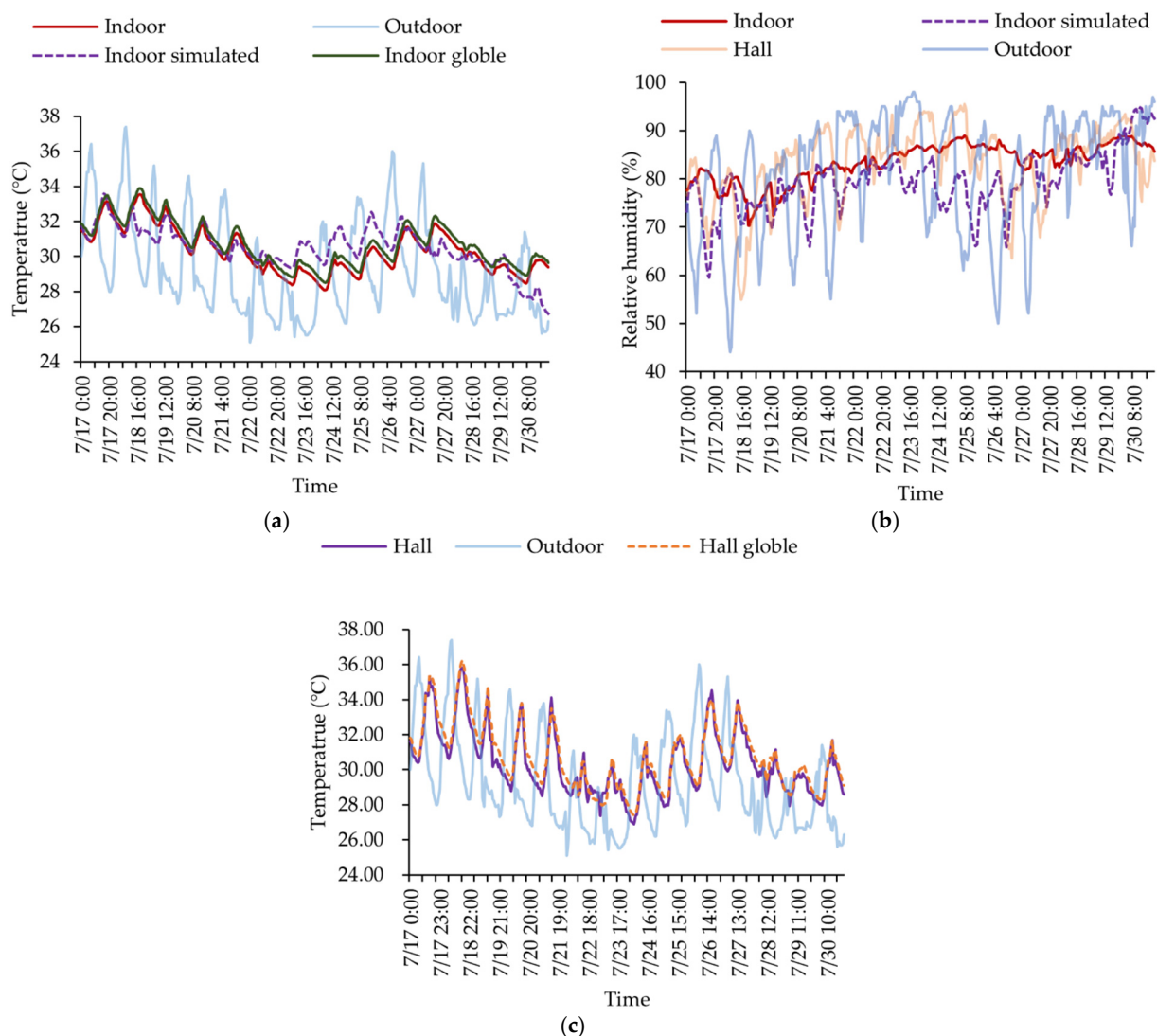


Figure 6. Comparison of measured and simulated values in summer: (a) Indoor temperature; (b) Relative humidity; (c) Hall temperature.

The weather station data of the city of Puning in 2019 was used as the weather input for building simulation. The variation trend of indoor air temperature predicted by simulation is consistent with the measured value, and it shows good prediction performance on sunny

days. The measured relative humidity is close to the simulated value, as shown in Figure 6b. Overall, the manually calibrated model can accurately simulate indoor temperature and relative humidity most of the time, with an average absolute error of 0.78 °C and 5.17%, respectively. Therefore, this model is deemed suitable for the simulation of an indoor thermal environment and further calculation of energy use if an HVAC system is applied to the house.

3.2. Heat Gain and Loss

The heat gain and loss of the envelope are simulated by feeding the typical meteorological year (TMY) data to the calibrated EnergyPlus model, assuming an HVAC system is installed and turned on. As can be seen from Figure 7, in summer, most of the heat gain of the house comes from the roof, and the maximum hourly heat gain can be reached at 4.93 kW. In winter, the heat loss of the roof is also larger than the floor and walls, with the maximum hourly heat loss in November of 3.34 kW. Affected by the ambient temperature and solar radiation, the wall is constantly being heated by solar heat gain from June to October, with a maximum hourly heat gain of 2.66 kW. The daily temperature is low in February and March, and the indoor air temperature is higher than the ambient temperature resulting in the wall being the heat-loss surface most of the time. Puning is located in hot summer and warm winter zone, and the summer is hot and long. The exterior rammed earth wall is a heated surface most of the time during the year, and the hourly mean heat gain is 0.41 kW. In addition, the heat transfer through the floor is also large, which is conducive to the passive cooling of the house during summer. From May to October, the floor always transfers heat to the ground with an average hourly heat loss of 2.25 kW. Thus, in summer, the floor is the heat loss surface, and the roof is the main heat gain surface. In winter, the roof is also the main heat gain surface, which potentially raises the indoor air temperature and creates a warm indoor environment for the occupants.

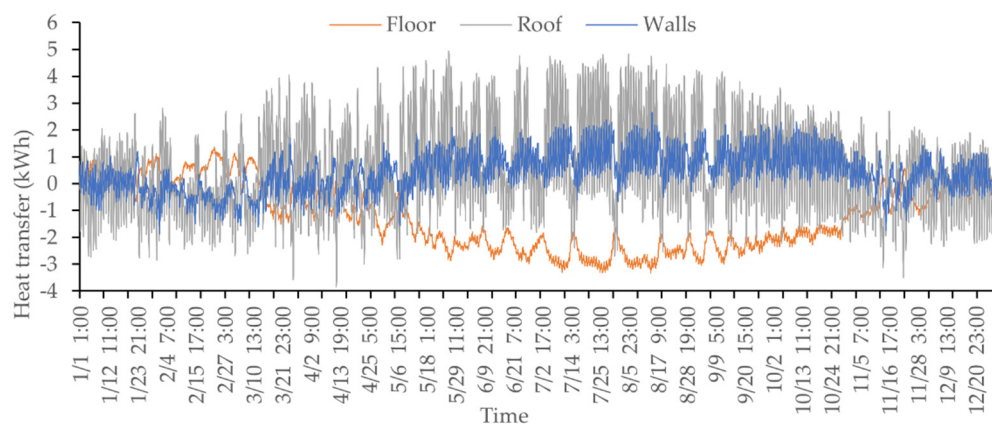


Figure 7. Hourly heat transfer of house envelope.

3.3. Indoor Thermal Comfort

3.3.1. Natural Ventilation

The hourly indoor environmental condition under natural ventilation conditions are simulated by DesignBuilder, and the simulated results are compared with the Chinese thermal comfort standard GB/T 50785-2012 “Civil Building Thermal and Humid Environment Evaluation Standard” [32] and the American ASHRAE 55-2017 standard [33]. The uncomfortable duration of the whole indoor thermal environment is shown in Figure 8. Under the provisions of the Chinese thermal comfort standard, the uncomfortable durations under the I and II levels are 3310 h and 829 h, respectively, accounting for 37.8% and 9.5% of the whole year. Under the ASHRAE 55-2017 standard, the duration of not meeting the acceptable ranges for 90% and 80% are 4418 h and 2984 h, respectively, which is longer than the uncomfortable duration calculated by the Chinese standard. Considering the differences in climate, culture, and physiology, this study adopts the Chinese thermal

comfort standard to evaluate indoor thermal comfort in Lingnan. Table 4 summarizes the uncomfortable durations for the four bedrooms under different criteria. Bedroom 1 has the best comfort, while bedroom 2 and bedroom 3 are less comfortable. On the whole, according to Chinese thermal comfort standard level II, the uncomfortable duration of each room is within 615~870 h. That is, the thermal comfort requirements are not met for about a month, and all of them appear in winter.

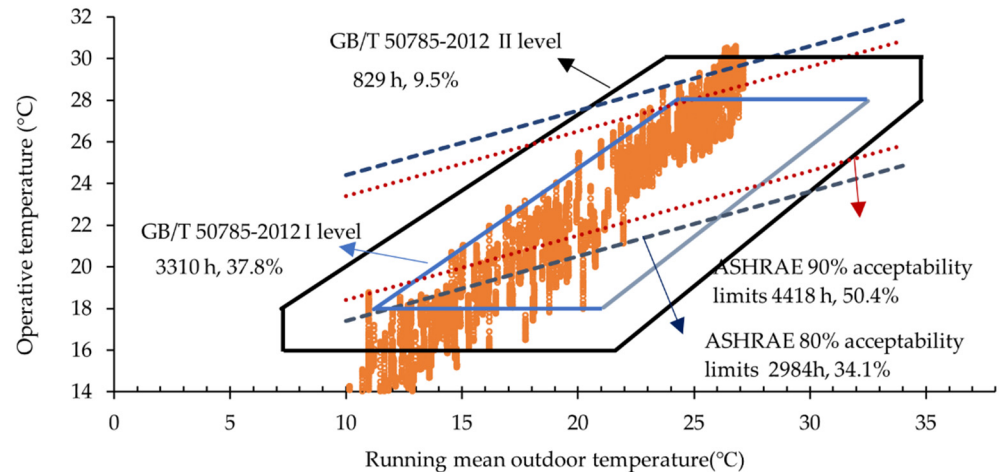


Figure 8. Overall indoor thermal comfort with natural ventilation.

Table 4. Uncomfortable durations with natural ventilation (unit: h).

Bedroom	GB/T 50785-2012		ASHRAE	
	I Level	II Level	90% Acceptability	80% Acceptability
1	2069	663	3847	2971
2	2567	870	4000	3126
3	2588	816	3881	3029
4	1852	615	3716	2777

The number of bedrooms corresponds to Figure 2.

3.3.2. HVAC

To further improve indoor thermal comfort, the bedroom thermal environment is simulated while the HVAC system is turned on. Indoor thermal comfort was evaluated by predicted mean vote (PMV). The clothing insulation of winter and summer is 1 clo and 0.5 clo, respectively, and the human metabolic index is 0.9. Figure 9 shows the changes in comfort indicators in each bedroom over time. It can be seen that about 95% of the time, the PMV is between -0.5 and 0.5 , and the corresponding predicted dissatisfaction percentage (PPD) is within 10%. Indoor PMV that does not meet the comfort range appeared in April, May, and November. PMV is between -0.85 and 0.85 about 99% of the time, and PPD is within 20%, which meets the requirements of human comfort.

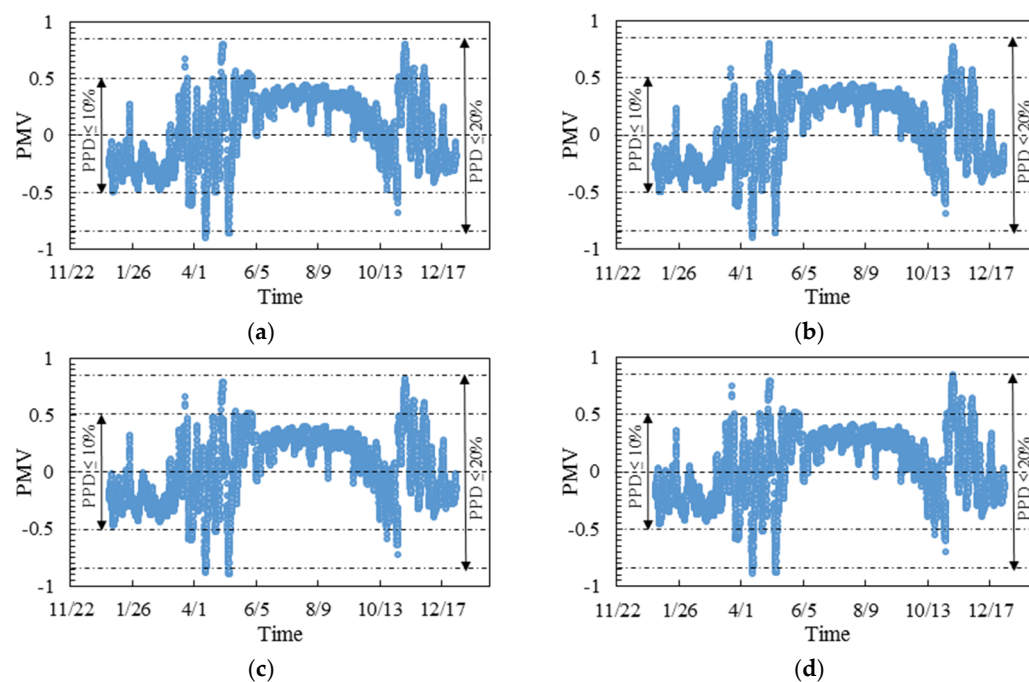


Figure 9. Bedroom thermal comfort with the HVAC system of (a) Bedroom 1; (b) Bedroom 2; (c) Bedroom 3; (d) Bedroom 4.

4. Retrofitting Measures

4.1. Energy Saving and Thermal Performance Retrofitting

From the heat gain and loss in Section 3.2, it can be known that in summer, heat is introduced into the room mainly through the roof and exterior walls, and the maximum hourly heat gain of the roof is close to 5 kW. Therefore, in summer, the optimization measures can be focused on improving the heat absorption by the roof. In winter, exterior walls are heat-loss surfaces most of the time because the indoor air temperature is higher than the ambient temperature. Therefore, in winter, the optimization measures can be focused on the exterior walls. Retrofitting measures of the envelope by reducing the roof heat gain and enhancing the wall insulation are included. In order to ensure that the original historical features of the “Four-point gold” are not damaged, an orthogonal experiment method is used to carry out the retrofitting. Natural ventilation, enhanced roof reflection and insulation, wall insulation, window shading, and carpet laying were selected as design variables. The orthogonal experiment design table of the retrofitting is shown in Table 5. The detail of the design rules and data processing method of the orthogonal experiments is shown in Appendix A.

Table 5. Factor-level table of the orthogonal experiment design of the retrofitting.

	Factors				
	Natural Ventilation	Heat-Reflective and Thermal Insulation Coating	Wall Insulation	Sunshade Width	Carpet
Level 1	Turn on	ZS-221 white	EPS(50 mm)	0.1 m	Carpet
Level 2	Turn off	Water-based	XPS(30 mm)	0.2 m	PVC carpet
Level 3		Cool glue	EPS(100 mm)	0.3 m	Textile carpet
Level 4		Kaisheng	XPS(50 mm)	0.4 m	
Level 5		RLHY-A05	EPS(20 mm)	0.5 m	

The physical properties of materials and construction costs of each measure are shown in Tables 6–8, respectively. Among them, carpets are only laid when the outdoor temper-

ature is below 15 °C, which is from 2 December to 4 March in the typical meteorological year. In this research, carpets, polyvinyl chloride (PVC) carpets, and textile carpets are considered. The expandable polystyrene (EPS) and extruded polystyrene (XPS) boards of different thicknesses are used for wall insulation with a heat conductivity coefficient of 0.8 W/(m·k) and 0.034 W/(m·k), respectively. To minimize the heat gain of the roof, five coatings with high thermal reflectivity, solar reflectivity, and hemispheric emissivity were considered. In addition, aluminum sunshades of different widths are planned to be installed above the east and west windows.

Table 6. Physical parameters and prices of wall insulation and carpet materials.

Component	Materials	Heat Conductivity Coefficient (W/(m·k))	Specific Heat (J/(kg·K))	Density (kg/m ³)	Unit Price (¥/m ²)	Area (m ²)	Total Price (¥)
Floor	Carpet	0.28	1000	290	16.33	179.6	2932.87
	PVC carpet	0.04	750	100	34.47	179.6	6190.81
	Textile carpet	0.06	1300	200	29.1	179.6	5226.36
Wall	EPS(50 mm)	0.8	1300	16	39	316	12,324
	XPS(30 mm)	0.034	1400	35	18	316	5688
	EPS(100 mm)	0.8	1300	16	78	316	24648
	XPS(50 mm)	0.034	1400	35	30	316	9480
	EPS(20 mm)	0.8	1300	16	15.6	316	4929.6

Table 7. Physical parameters and prices of heat-reflective and thermal insulation coating of roof.

Coating	Thermal Reflectivity	Tolar Reflectivity	Hemispheric Emissivity	Unit Price (¥/m ²)	Area (m ²)	Total Price (¥)
ZS-221	0.92	0.88	0.89	7.5	232.8	1746
Water-based	0.9	0.91	0.93	8.75	232.8	2037
Cool glue	0.85	0.89	0.89	4.25	232.8	989.4
Kaisheng	0.85	0.85	0.88	7.5	232.8	1746
RLHY-A05	0.92	0.95	0.9	7.5	232.8	1746

Table 8. Widths and prices of aluminum panel.

Width(m)	Unit Price (¥/m ²)	Area (m ²)	Total Price (¥)
0.1	72	0.406	29.232
0.2	72	0.812	58.464
0.3	72	1.218	87.696
0.4	72	1.624	116.928
0.5	72	2.03	146.16

When the indoor temperature is 2 °C higher than the outdoor temperature, natural ventilation is used for cooling. The HVAC system is activated only when natural ventilation is insufficient to maintain comfort. The operating hours coincide with the rest period of the occupants, from 22:00 to 9:00 the next morning. In addition, the compressor was placed at the window on the second floor in conjunction with the bedroom layout of a traditional rammed house and its storage space on the second floor, which allows for more comfortable living conditions without destroying the historic character. Last but not least, the whole house is retrofitted, but the HVAC system was only used in the four bedrooms.

4.2. Sensitivity Analysis of Retrofitting Measures

4.2.1. Energy Saving

The annual HVAC energy consumption before the retrofitting of the rammed earth house was calculated to be 4695.62 kWh, which was used as the benchmark for calculating energy savings. After taking retrofitting measures, the total energy consumption was significantly reduced. The sensitivity analysis of each energy-saving retrofitting measure is shown in Table 9. The maximum average energy saving in the orthogonal experiment is 2192.27 kWh/a. The maximum difference for energy saving of wall insulation, heat-reflective and thermal insulation coating, sunshade width, natural ventilation, and carpet is 1294.96 kWh/a, 197.49 kWh/a, 159.96 kWh/a, 91.51 kWh/a and 79.53 kWh/a, respectively. Therefore, the impact of each retrofitting measure on energy savings can be ranked as follows: wall insulation, heat-reflective and thermal insulation coating, sunshade width, natural ventilation, and carpet. Among wall insulations, the energy-saving effect of level 4 (XPS 50 mm) is higher than other wall insulation materials. For heat-reflective and thermal insulation coatings and sunshade width, the energy-saving effect of level 5 coating material (RLHY-A05) and level 5 sunshade width (0.5 m) is better than other measures in each group. For natural ventilation and carpets, turning off the window (door) and PVC carpet have better performance in energy saving compared with other measures. To sum up, the combined design of 50 mm XPS panel, RLHY-A05 coating, 0.5 m sunshade width, turning off the window (door), and PVC carpet can be considered as the optimal scheme for energy saving.

Table 9. Sensitivity analysis of the energy saving.

		Factors				
		Natural Ventilation	Heat-Reflective and Thermal Insulation Coating	Wall Insulation	Sunshade Width	Carpet
$\overline{K_{jm}}$	Level 1	1358.55	1395.93	1138.04	1278.21	1413.01
	Level 2	1450.05	1444.99	1888.74	1422.72	1430.45
	Level 3		1288.47	873.58	1409.33	1350.92
	Level 4		1360.40	2168.54	1427.32	
	Level 5		1485.96	906.85	1438.17	
R_j		91.51	197.49	1294.96	159.96	79.53
Rank of impact level		Wall insulation > Heat-reflective and thermal insulation coating > Sunshade width > Natural ventilation > Carpet				
Best scheme		2	5	4	5	2

4.2.2. Economic Performance

The study has shown that the total cost of retrofitting measures is approximately 1.2–1.5 times the cost of energy-saving materials [34]. Therefore, the total cost of each retrofitting measure can be calculated based on the unit price and area of each material shown in Tables 6–8. In this research, the dynamic investment payback period was selected as the criteria to evaluate the economic performance of each retrofitting measure. The sensitivity analysis of the dynamic investment payback period for each retrofitting measure is shown in Table 10. Natural ventilation can be achieved by manually opening windows and doors without investment costs. Therefore, there is no need to discuss the economic performance of natural ventilation. The minimum average dynamic investment payback period in the orthogonal experiment is 9.17 years. When EPS materials are used, the dynamic investment payback period cannot be calculated. The maximum differences for a dynamic investment payback period of sunshade, carpet, and coating are 2.99, 2.86, and 2.83, respectively. Therefore, the impact of each retrofitting measure on the dynamic investment payback period can be ranked in order as follows: wall insulation, sunshade width, carpet, and heat-reflective and thermal insulation coating. For wall insulation, the economic performance of level 2 (XPS 30 mm) is better than other wall insulation materials. Among all heat-reflective and thermal insulation coatings, the water-based coating has the

best economic performance. For carpets, the economic performance of the carpet is the best. For sunshade width, the 0.5 m sunshade width has the best performance in economic performance. In general, the combined design of 30 mm XPS panel, water-based coating, carpet, and 0.5 m sunshade width can achieve optimal economic performance.

Table 10. Sensitivity analysis of the dynamic investment payback period.

		Factors				
		Natural Ventilation	Heat-Reflective and Thermal Insulation Coating	Wall Insulation	Sunshade Width	Carpet
$\overline{K_{jm}}$	Level 1	N/A	6.47	N/A	8.07	4.29
	Level 2	N/A	5.33	15.97	6.58	7.12
	Level 3		8.16	N/A	7.04	7.15
	Level 4		6.85	16.86	6.07	
	Level 5		6.02	N/A	5.07	
R_j		N/A	2.83	N/A	2.99	2.86
Rank of impact level		Wall insulation > Sunshade width > Carpet > Heat-reflective and thermal insulation coating				
Best scheme		N/A	2	2	5	1

4.2.3. Indoor Thermal Environment

The annual indoor unacceptable thermal comfort hours of the rammed earth house are selected as the criteria to evaluate the indoor thermal environment improvement. The sensitivity analysis of the annual indoor unacceptable thermal comfort hours for each retrofitting measure is shown in Table 11. The maximum average annual indoor unacceptable thermal comfort hours in the orthogonal experiment is 1766 h. The maximum difference for the annual indoor unacceptable thermal comfort hours of wall insulation, heat-reflective and thermal insulation coating, sunshade width, carpet, and natural ventilation is 276.60 h, 253.00 h, 116.80 h, 85.50 h, and 5.37 h, respectively. Therefore, the impact of each retrofitting measure on the annual indoor unacceptable thermal comfort hours can be ranked in positive order as follows: wall insulation, heat-reflective, and thermal insulation coating, sunshade width, carpet, and natural ventilation. Among wall insulations, the annual indoor unacceptable thermal comfort hours of level 3 (EPS 100 mm) are higher than other wall insulation materials. For all heat-reflective and thermal insulation coatings, ZS-221 white coating results in the largest increase in the annual indoor thermal comfort period. For carpets, the annual indoor unacceptable thermal comfort hours of the textile carpet are the longest. For the sunshade width, the 0.3 m sunshade width has the best performance for the annual indoor unacceptable thermal comfort hours. For natural ventilation, opening windows (doors) can have the best performance in shrinking the annual indoor unacceptable thermal comfort hours. In general, the combined design of 100 mm EPS panel, ZS-221 white coating, textile carpet, 0.3 m sunshade width, and opening windows (doors) can achieve the optimal scheme for the indoor thermal environment.

Table 11. Sensitivity analysis of the annual indoor unacceptable thermal comfort hours.

		Factors				
		Natural Ventilation	Heat-Reflective and Thermal Insulation Coating	Wall Insulation	Sunshade Width	Carpet
$\overline{K_{jm}}$	Level 1	1243.47	1322.00	1258.80	1217.40	1199.40
	Level 2	1238.10	1204.20	1173.20	1208.00	1218.70
	Level 3		1307.20	1382.00	1324.80	1284.90
	Level 4		1304.20	1105.40	1225.00	
	Level 5		1069.00	1287.20	1231.40	
R_j		5.37	253.00	276.60	116.80	85.50
Rank of impact level		Wall insulation > Heat-reflective and thermal insulation coating > Sunshade width > Carpet > Natural ventilation				
Best scheme		1	1	3	3	3

4.3. Optimized Scheme

The above retrofitting schemes focus on a single optimization objective without considering the combined impact of various measures on building energy consumption, economic performance, and the indoor thermal environment. However, various retrofitting measures will be applied simultaneously for a single building. Therefore, it is necessary to propose a comprehensively optimized scheme which can be used in the actual retrofitting. The K-means clustering algorithm is used to find the comprehensively optimized scheme. According to the results of the dynamic investment payback period, different indicators of twenty-five cases in Appendix A are divided into eleven grades, and the number 11 represents the best grade. The comprehensive indicator is the sum of grade values for energy saving, economic performance, and indoor thermal environment. The sensitivity analysis of the comprehensively optimized scheme is shown in Table 12. The maximum difference for the performance of the comprehensively optimized scheme of wall insulation, heat-reflective and thermal insulation coating, sunshade width, carpet, and natural ventilation is 10.00, 3.60, 1.80, 1.50, and 1.13, respectively. Therefore, the impact of each retrofitting measure on the performance of the comprehensively optimized scheme can be ranked in positive order as follows: wall insulation, heat-reflective and thermal insulation coating, sunshade width, carpet, and natural ventilation. Among them, 30 mm XPS, ZS-221 white coating, carpet, 0.5 m sunshade width, and turning off windows (doors) can be regarded as the combined design to achieve the comprehensively optimized scheme.

Table 12. Sensitivity analysis of the comprehensively optimized scheme.

		Factors				
		Natural Ventilation	Heat-Reflective and Thermal Insulation Coating	Wall Insulation	Sunshade Width	Carpet
$\overline{K_{jm}}$	Level 1	15.67	17.80	14.00	15.20	17.00
	Level 2	16.80	16.40	21.80	15.20	15.50
	Level 3		15.60	11.80	16.60	16.30
	Level 4		16.60	21.20	16.60	
	Level 5		14.20	11.80	17.00	
R_j		1.13	3.60	10.00	1.80	1.50
Rank of impact level		Wall insulation > Heat-reflective and thermal insulation coating > Sunshade width > Carpet > Natural ventilation				
Best scheme		2	1	2	5	1

In summary, improving wall insulation is the most effective way for energy saving and indoor thermal comfort mitigation, but EPS is too expensive for the dynamic investment payback period. Heat-reflective and thermal insulation coating and sunshades with low initial investments also have good performance in reducing the heat gains from solar radiation, resulting in lower energy consumption and longer comfort period. Carpet is only used in winter, so the annual benefits can be relatively insignificant. Moreover, the enhancement of natural ventilation has not yielded desired effect because the transition season in this climate is short. Based on the comprehensive index, 30 mm XPS wall insulation, ZS-221 heat-reflective and thermal insulation coating, sunshade width of 0.5 m, carpet, and natural ventilation are a recommended retrofitting scheme.

5. Conclusions

This study analyzed the thermal performance and environment of traditional rammed earth houses in Lingnan, south China. Energy-saving retrofitting measures are proposed to improve the indoor thermal environment by taking the building conditions and local customs into account. It not only retains the historical features and cultural value of traditional rammed earth houses but also improves thermal comfort and achieves energy saving.

The heat transfer of rammed earth houses behaves differently by seasons. In summer, most of the heat gain comes from the roof and exterior walls. During winter, the heat loss is

mainly due to the exterior walls. Hence, the retrofitting measures mainly focus on reducing the heat gain of the roof and enhancing the insulation of the wall.

Five energy-saving retrofitting measures, comprised of natural ventilation, enhanced roof reflection and insulation, wall insulation, window shading, and carpet laying, are proposed. The highest performance of retrofitting scheme on energy saving, dynamic investment payback period, and the annual indoor thermal comfort increase table are 2192.27 kWh/a, 9.17 years, and 1766 h, respectively. The research puts forward a comprehensively optimized scheme, which consists of 30 mm XPS 30 mm, ZS-221 white coating, carpet, 0.5 m sunshade width, and turning off windows (doors). The optimized scheme can be practically used in renovation, which balances energy saving, economic performance, and indoor thermal environment.

6. Limitations

This work takes the “four-point gold” house as a sample to analyze its thermal performance and search for a suitable retrofitting scheme. The conclusions and the application of retrofitting measures are limited to this specific type of traditional rammed earth residential buildings in the Lingnan region, and it is also one of the most popular types. We will study other types of traditional rammed earth buildings in the future and achieve more universal and comprehensive results for the traditional residential houses in the region.

Author Contributions: Conceptualization, S.L. and M.W.; methodology, P.S.; software, S.L., L.Z. and C.W.; validation, X.C., C.W. and L.B.; formal analysis, X.C., L.B. and R.W.; investigation, P.S.; resources, P.S.; data curation, M.W. and L.Z.; writing—original draft preparation, S.L. and M.W.; writing—review and editing, X.C., P.S. and M.W.; visualization, R.W.; supervision, P.S.; project administration, P.S.; funding acquisition, P.S. All authors have read and agreed to the published version of the manuscript.

Funding: This research was funded by the National Natural Science Foundation of China (NSFC) [Grant number. 52008132]; Harbin Institute of Technology (Shenzhen) Innovation Research Course Construction Project; and Shenzhen Science and Technology Program [Grant number. RCBS202007141 14921062].

Institutional Review Board Statement: Not applicable.

Informed Consent Statement: Not applicable.

Data Availability Statement: Not applicable.

Conflicts of Interest: The authors declare no conflict of interest.

Appendix A

Table A1. Orthogonal experiment table.

Case	Factors								Comprehensive Indicator
	Natural Ventilation	Roof Reflection	Thermal Insulation	Sunshade Width	Carpet	Energy Saving (kWh/a)	Dynamic Investment Payback Period Year	Annual Indoor Unacceptable Thermal Comfort Hours h	
1	1	1	1	1	1	1083.34	N/A	1361	16
2	1	2	2	2	2	2032.26	14.83	1110	20
3	1	3	3	3	3	847.24	N/A	1766	14
4	1	4	4	4	4(2)	2157.65	21.19	1244	21
5	1	5	5	5	5(3)	991.42	N/A	1176	10
6	2	1	2	3	4(2)	2035.69	14.27	1307	25
7	2	2	3	4	5(3)	909.33	N/A	1305	12
8	2	3	4	5	1	2192.27	12.29	1071	23
9	2	4	5	1	2	833.85	N/A	1307	11
10	2	5	1	2	3	1227.55	N/A	1110	12
11	3(1)	1	3	5	2	838.8	N/A	1351	13
12	3(1)	2	4	1	3	2150.63	11.82	1074	24
13	3(1)	3	5	2	4(2)	900.47	N/A	1290	12
14	3(1)	4	1	3	5(3)	1034.91	N/A	1341	15
15	3(1)	5	2	4	1	2049.45	9.17	963	23
16	4(2)	1	4	2	5(3)	2175.06	18.07	1226	22
17	4(2)	2	5	3	1	961.73	N/A	1298	13
18	4(2)	3	1	4	2	1173.4	N/A	1248	14
19	4(2)	4	2	5	3	1997.36	13.08	1325	26
20	4(2)	5	3	1	4(2)	994.28	N/A	1184	10
21	5(1)	1	5	4	3	846.76	N/A	1365	13
22	5(1)	2	1	5	4(2)	1170.98	N/A	1234	13
23	5(1)	3	2	1	5(3)	1328.95	28.51	1161	15
24	5(1)	4	3	2	1	778.24	N/A	1304	10
25	5(1)	5	4	3	2	2167.08	20.95	912	16

References

1. Minke, G. *Building with Earth: Design and Technology of a Sustainable Architecture*; Birkhäuser: Basel, Switzerland, 2012.
2. Jaquin, P.A.; Augarde, C.E.; Gerrard, C.M. Chronological description of the spatial development of rammed earth techniques. *Int. J. Archit. Herit.* **2008**, *2*, 377–400. [[CrossRef](#)]
3. Arrigoni, A.; Beckett, C.; Ciancio, D.; Dotelli, G. Life cycle analysis of environmental impact vs. durability of stabilised rammed earth. *Constr. Build. Mater.* **2017**, *142*, 128–136. [[CrossRef](#)]
4. Reddy, B.V.V.; Kumar, P.P. Embodied energy in cement stabilised rammed earth walls. *Energy Build.* **2010**, *42*, 380–385. [[CrossRef](#)]
5. Venkatarama Reddy, B.V.; Leuzinger, G.; Sreeram, V.S. Low embodied energy cement stabilised rammed earth building—A case study. *Energy Build.* **2014**, *68*, 541–546. [[CrossRef](#)]
6. Strazzeri, V.; Karrech, A. Energy and thermal performance of a typical rammed earth residential building in Western Australia. *Energy Build.* **2022**, *260*, 111901. [[CrossRef](#)]
7. Fernandes, J.; Mateus, R.; Gervásio, H.; Silva, S.M.; Bragança, L. Passive strategies used in Southern Portugal vernacular rammed earth buildings and their influence in thermal performance. *Renew. Energy* **2019**, *142*, 345–363. [[CrossRef](#)]
8. Soudani, L.; Woloszyn, M.; Fabbri, A.; Morel, J.-C.; Grillet, A.-C. Energy evaluation of rammed earth walls using long term in-situ measurements. *Sol. Energy* **2017**, *141*, 70–80. [[CrossRef](#)]
9. Soebarto, V. Analysis of indoor performance of houses using rammed earth walls. In Proceedings of the Eleventh International IBPSA Conference, Glasgow, Scotland, 27–30 July 2009; pp. 1530–1537.
10. Dong, X.; Soebarto, V.; Griffith, M. Strategies for reducing heating and cooling loads of uninsulated rammed earth wall houses. *Energy Build.* **2014**, *77*, 323–331. [[CrossRef](#)]
11. Taylor, P.; Fuller, R.J.; Luther, M.B. Energy use and thermal comfort in a rammed earth office building. *Energy Build.* **2008**, *40*, 793–800. [[CrossRef](#)]
12. Beckett, C.; Cardell-Oliver, R.; Ciancio, D.; Huebner, C. Measured and simulated thermal behaviour in rammed earth houses in a hot-arid climate. *Part B Comfort. J. Build. Eng.* **2017**, *13*, 146–158.
13. Xiang, D.; Soebarto, V.; Griffith, M. Achieving thermal comfort in naturally ventilated rammed earth houses. *Build. Environ.* **2014**, *82*, 588–598.
14. Dong, X.; Soebarto, V.; Griffith, M. Design optimization of insulated cavity rammed earth walls for houses in Australia. *Energy Build.* **2015**, *86*, 852–863. [[CrossRef](#)]
15. Giuffrida, G.; Detommaso, M.; Nocera, F.; Caponetto, R. Design optimisation strategies for solid rammed earth walls in Mediterranean climates. *Energies* **2021**, *14*, 325. [[CrossRef](#)]
16. Fernandes, J.; Pimenta, C.; Mateus, R.; Monteiro Silva, S.; Bragança, L. Contribution of Portuguese Vernacular Building Strategies to Indoor Thermal Comfort and Occupants' Perception. *Buildings* **2015**, *5*, 1242–1264. [[CrossRef](#)]
17. Fernandes, J.; Mateus, R.; Braganca, L.; Silva, J.J.C.D. Portuguese vernacular architecture: The contribution of vernacular materials and design approaches for sustainable construction. *Archit. Sci. Rev.* **2015**, *58*, 324–336. [[CrossRef](#)]
18. Martin, S.; Mazarron, F.R.; Canas, I. Study of thermal environment inside rural houses of Navapalos (Spain): The advantages of reuse buildings of high thermal inertia. *Constr. Build. Mater.* **2010**, *24*, 666–676. [[CrossRef](#)]
19. Priya, R.S.; Sundarraja, M.C.; Radhakrishnan, S.; Vijayalakshmi, L. Solar passive techniques in the vernacular buildings of coastal regions in Nagapattinam, TamilNadu-India—a qualitative and quantitative analysis. *Energy Build.* **2012**, *49*, 50–61. [[CrossRef](#)]
20. Saljoughinejad, S.; Sharifabad, S.R. Classification of climatic strategies, used in Iranian vernacular residences based on spatial constituent elements. *Build. Environ.* **2015**, *92*, 475–493. [[CrossRef](#)]
21. Fernandes, J.; Mateus, R.; Braganca, L. The Potential of Vernacular Materials to the Sustainable Building Design. In Proceedings of the International Conference on Vernacular Heritage and Earthen Architecture (CIAV)/VerSus/7th ATP, Vila Nova de Cerveira, Portugal, 16–20 October 2013; pp. 623–629.
22. Singh, M.K.; Mahapatra, S.; Atreya, S.K. Solar passive features in vernacular architecture of North-East India. *Sol. Energy* **2011**, *85*, 2011–2022. [[CrossRef](#)]
23. Gu, Y.; Xu, H. Spatial Representation of Rural Clan-Organized Society Structure: The Case of Chaoshan Culture Area. *Urban Plan. Forum* **2017**, *3*, 103–109.
24. Archaic Pashi House. Available online: <http://dz.cppfoto.com/activity/showG.aspx?works=1807770&page=1> (accessed on 4 January 2022).
25. Zeng, Z.; Li, L.; Pang, Y. Analysis on climate adaptability of traditional villages in Lingnan, China—World Cultural Heritage Site of Majianglong Villages as example. *Procedia Eng.* **2017**, *205*, 2011–2018. [[CrossRef](#)]
26. Li, Q.; You, R.; Chen, C.; Yang, X. A field investigation and comparative study of indoor environmental quality in heritage Chinese rural buildings with thick rammed earth wall. *Energy Build.* **2013**, *62*, 286–293. [[CrossRef](#)]
27. Zhang, W.; Chen, Z. Studies on Optimization and Integration of Photovoltaics in traditional Lingnan buildings: A case study in Guangzhou. *Procedia Eng.* **2017**, *205*, 3003–3010. [[CrossRef](#)]
28. Mazzarella, L. Energy retrofit of historic and existing buildings. The legislative and regulatory point of view. *Energy Build.* **2015**, *95*, 23–31.
29. Healy, S. Air-conditioning and the 'homogenization' of people and built environments. *Build. Res. Inf.* **2008**, *36*, 312–322. [[CrossRef](#)]

30. China Development and Reform Commission. *Construction Project Economic Evaluation Approaches and Parameters*; China Plan Press: Beijing, China, 2006.
31. Jain, A.K. Data Clustering: 50 Years Beyond K-means. *Pattern Recognit. Lett.* **2010**, *31*, 651–666. [[CrossRef](#)]
32. Ministry of Housing and Urban-Rural Development. *Civil Building Thermal and Humid Environment Evaluation Standard*; China Construction Industry Press: Beijing, China, 2012; pp. 5–10.
33. *ANSI/ASHRAE Standard 55-2017*; Thermal Environmental Conditions for Human Occupancy. ASHRAE: Atlanta, GA, USA, 2017; pp. 4–18.
34. Li, Z.; Wang, Z.Z.; Sun, Y.; Shao, Z.B. Economic Evaluation of Energy Saving Technology for Building Envelope: Taking a residential building in Henan as an example. *Build. Energy Effic.* **2017**, *7*, 123–126. [[CrossRef](#)]